JOURNAL OF CATALYSIS 127, 744–760 (1991)

Studies on Chromia/Zirconia Catalysts

I. Preparation and Characterization of the System

A. CIMINO, D. CORDISCHI, S. DE ROSSI, G. FERRARIS, D. GAZZOLI, V. INDOVINA, G. MINELLI, M. OCCHIUZZI, AND M. VALIGI

Centro di Studio SACSO CNR, % Dipartimento di Chimica, Università La Sapienza, 00185 Roma, Italy

Received January 2, 1990; revised June 18, 1990

The preparation and characterization (chemical, textural, DTA, XRD, XPS) of chromium oxide/zirconia, of interest as hydrogenation catalysts, are reported. The support (obtained via $ZrOCl_2$ hydrolysis) can be tailored in surface area from high (360 m^2g^{-1}) to low (about 20 m^2g^{-1}) values, and in texture from microporous to mesoporous and macroporous according to the treatment temperature (from 383 to 923 K) of the starting "hydrous zirconia." By contacting the support with Cr(VI) solution, chromium-loaded specimens, ZC, are prepared. The Cr uptake is roughly constant (1.5 to 1.9 Cr atoms nm^{-2}) for zirconia previously heated at $T \geq 573$ to 923 K. Higher loadings can be reached on the hydrous zirconia. Supported Cr oxide is an effective antisintering agent for zirconia, and it also opposes the tetragonal → monoclinic transition. By subjecting the ZC specimens to various heat and redox treatments, the average oxidation number of Cr, $\bar{n}$, changes. From an initial value of +6, $\bar{n}$ decreases to +5.5 after oxygen treatment at 773 K, to +2.5 after CO treatment at 623 K, and can be restored to +5.5 if the sample is reoxidized in oxygen at 773 K. Treatment in H_2O vapor at 723 K of a reduced ($\bar{n}$ = 2.5) specimen brings $\bar{n}$ to 3.0. The existence of Cr(VI), Cr(V), Cr(III), and Cr(II) is inferred and is supported by XPS analysis. A separate paper presents an ESR investigation and discusses the nature of the surface Cr species.

INTRODUCTION

Supported chromium ions are known to possess important catalytic properties, but they have been studied mainly on silica and alumina (1–4). Zirconia has been investigated as a support in recent years, but to an extent not comparable to silica or alumina, and little work has specifically dealt with supported chromia. It is well known that the dispersion, the oxidation state, and the structural features of the supported ions may strongly depend on the support. A program has accordingly been started to study the chromia/zirconia system, aiming at correlating catalytic properties, notably in hydrogenation and dehydrogenation reactions, with the surface chemistry of chromia/zirconia catalysts. A communication reporting the catalytic activity for the H_2–D_2 equilibration as well as a few preliminary results of the study of some surface features has been given before (*5*). The present paper (Part I) describes the preparation and characterization of the catalysts. Attention is given mainly to textural features of the support, and to dependence upon Cr addition. Chemical, DTA, X-ray, and XPS techniques are employed. Since the samples are treated at different temperatures in oxygen or in a reducing atmosphere the state of chromium, initially present as Cr(VI) species, changes and investigations of this process by chemical, redox, and XPS techniques are reported. A subsequent paper (Part II) based on an ESR study examines in detail the complex problem of the identification and quantification of the Cr species generated by various treatments. The catalytic activity of chromia/zirconia for propene hydrogena-

0021-9517/91 $3.00

tion is presented in a third paper (Part III) which shows the type of correlation found between Cr species and catalytic activity. Some results of an IR study in correlation with an ESR and catalytic investigation have been presented elsewhere (6).

EXPERIMENTAL

Sample Preparation

The starting material for the preparation of zirconia and of the chromium-containing specimens was a hydrous zirconium oxide obtained by precipitation from $ZrOCl_2$ solutions. The precipitation was carried out by bubbling a stream of ammonia-saturated nitrogen for 24 h into a $ZrOCl_2$ solution (final pH 10). The precipitate was washed with water until the Cl^- test (addition of $AgNO_3$ to a small portion of the liquid) gave no visible opalescence, a process which required about 8 h. Some preparations involved a much longer rinsing time, from 48 to 72 h, to remove Cl^- as measured in the solid. The precipitate was thereafter dried at 383 K for 24 h (first heat treatment). Other zirconium oxides with different textural properties were prepared by subjecting the above material to a final thermal treatment in the range 573 to 1023 K in air for 5 h. All zirconium oxide specimens are designated as $ZrO_2(T)$, where T is the temperature of the final heating treatment in air. Thus, for example, the above material simply dried at 383 K is referred to as $ZrO_2(383)$.

The chromium-containing samples were prepared by bringing into contact about 10 g of $ZrO_2(T)$ with a large volume (usually 250 cm^3) of a titrated solution of chromium trioxide, in accordance with the principle illustrated by Li Wang and Hall (7). In the case of $ZrO_2(383)$, the influence of pH on the chromium uptake was studied in preliminary experiments. To this end, the final pH was kept strongly acid in two series (pH 1.0 and 1.5) by HNO_3 addition, or slightly basic (pH 8.5) by ammonia addition in a third series. The chromium uptake could then be followed as a function of time, by analyzing a small volume of the contacting solution (0.25 cm^3) and hence calculating the Cr captured by the solid. The influence of pH and the progress of uptake with time are shown in Fig. 1, A time of 72 h was seen to be sufficient to reach equilibrium. On the basis of the higher Cr uptake in the acid solution, pH 1 and 72 h contact time were adopted as a standard procedure for the preparation. Different Cr contents (wt%) could be obtained by varying the concentration of the contacting solution, and/or by varying the temperature T to which the starting hydrous oxide $ZrO_2(383)$ was subjected, and therefore selecting materials with different textures. After impregnation, portions of the specimens were subjected to different heat treatments in air or in oxygen, as specified below.

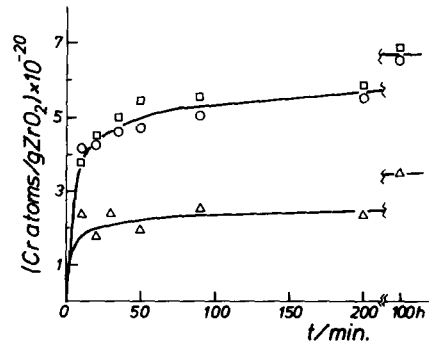

FIG. 1. Chromium uptake by hydrous zirconium oxide vs time in acid (○, pH 1; □, pH 1.5) or basic (△, pH 8.5) conditions.

Chromium-containing samples are designated as $ZCx(T)$, where x is the approximate Cr metal content (wt%) and T is the temperature to which the starting zirconium oxide was subjected before chromium uptake, that is, the T value appearing in the symbol $ZrO_2(T)$ of the material used. Capital letters after (T) refer to distinct preparations of the support. Independent preparations leading to similar Cr content starting from the same zirconia batch are distinguished by asterisks (*).

Chemical Analysis

The Cr content of all specimens after impregnation and drying at 383 K was analyzed by dissolving a known amount of the solid in hot concentrated H_2SO_4. After cooling and dilution the solution was analyzed by atomic absorption (AA), using Zr(IV)-containing chromium standards, having a Zr content (as sulphate) comparable to the analyzed solution. For some specimens a check of the Cr balance between solid and solution at the end of the contact time was made, with satisfactory results. The direct analysis of Cr in the solid, however, proved to be more reliable than the indirect assessment from the analysis of the solution, and it is this former value which is reported under Results. Specimens subjected to heat treatment in air or in oxygen required preliminary fusion with $KHSO_4$ in order to dissolve the solid.

The Cl analysis was performed by the Volhard method (*8*). The samples (0.5 g) were dissolved in a 40% HF solution (1 ml). After dilution to 15 ml, 5 ml of HNO_3 (16 *M*) and 2 g of $NH_4Fe(SO_4)_2 \cdot 10\ H_2O$ were added. This large amount of iron salt was necessary to compensate for the decrease in the concentration of Fe^{3+} ions due to the formation of the very stable FeF_6^{3-} complex (*9*). The Cl^- determination was accomplished by back-titrating a known volume of a standardized $AgNO_3$ solution (0.1 *M*) by a standardized KCNS solution.

Heat Treatments and the State of Chromium

The main interest of the present study is focused on the heat-treated Cr-containing samples, especially as regards their surface and catalytic behavior. Thermal treatments of ZC*x*(*T*) samples was carried out in air or in dry oxygen. The treatment in dry oxygen at 773 K, usually adopted, is referred to as "standard oxidation" (s.o.). All treatments in air or oxygen caused a change of color, and analyses showed that the chromium was partially reduced. The fraction of Cr(VI) still present was analyzed by bringing the solid into contact with a 10 *M* NaOH solution, heated to incipient boiling for 0.5 h. After cooling, the suspension was centrifuged and filtered and the solution pH adjusted to 2 by addition of H_2SO_4 for atomic absorption analysis. To check that chromium oxidation during the NaOH extraction in air did not affect the results, aliquots of a specimen ZC6(383)A subjected to s.o. were contacted with NaOH in air for different times (0.2, 0.5, and 1 h) or with NaOH in a nitrogen atmosphere for 0.5 h. In all cases, the Cr(VI) content was the same, within the experimental error. In some cases, in addition to the AA (total) Cr analysis of the extracted Cr, a specific test for Cr(VI) was made in two ways: (i) spectrophotometrically (SP), at $\lambda = 349$ nm (*10*), and (ii) titrimetrically (TM), by a standardized Fe(II) solution (*11*). The results of the three methods agree, as shown by the example in the following two sets: ZC1(383)A: 0.55 (AA), 0.49 (SP), 0.52 (TM); ZC2(383)A, 1.07 (AA), 0.93 (SP), 1.01 (TM). The determination by AA was more reliable and practical, and was adopted thereafter.

Surface Area and Porosimetry

The surface areas (SA) of all samples were measured by N_2 adsorption at 77 K (BET method). Pore size distributions and related mesopore cumulative volumes were determined from the corresponding nitrogen adsorption–desorption isotherms at 77 K, according to the Brunauer–Mikhail-Bodor "corrected modelless" method (*12*) applied to the desorption branch. For the correction terms the parallel-plate hypothesis for pore shape has been assumed. Total pore volumes were calculated from the respective isotherms at $p/p_0 = 0.95$ by assuming the Gurvitsch rule and taking the appropriate liquid density (*13*). Specific surface areas, S_t, were obtained, by the *t*-plot method (*14*), using the standard isotherms of similar C_{BET} values, given by Lecloux and Pirard (*15*).

X-Ray Diffraction

The identification of phases was carried out by means of a Philips PW 1725 diffractometer, employing Cu$K\alpha$ (Ni-filtered) radiation. The relative amounts of the tetragonal (t) and monoclinic (m) phases were evaluated by intensity measurements of (111) and ($11\bar{1}$) reflections for m and (101) for t, indexed according to Teufer (*16*). The intensity was measured by registration of the reflections and by a cut and weigh procedure of the peaks recorded on paper.

DTA Determinations

DTA measurements were performed by a Perkin–Elmer apparatus from room temperature to 1173 K in flowing N_2 or O_2 (60 ml/min), using-α-Al_2O_3 as reference, and a temperature rise rate of 20 K/min. For each experiment the charge of the sample (typically 35 mg) was covered with 15 mg of α-Al_2O_3. The sample and the reference, of comparable volumes, were placed in platinum containers. To evaluate the intensity of the thermal effects, the peaks were reproduced on paper and their area measured by a cut and weigh procedure.

Redox-Cycles

The experiments were performed in a circulation all-glass apparatus connected to a mass spectrometer (VG Micromass 601). The apparatus was equipped with a magnetically driven pump (flow rate about 0.8 liter min^{-1}), a pressure transducer (MKS Baratron, sensitivity 1 Pa), a silica reactor containing the sample (0.3 to 0.5 g) placed on a fritted disk, and a trap at 77 K placed downstream from the reactor. The reduction–oxidation cycles consisted of (i) 0.5 h evacuation at 383 K, (ii) heating in oxygen at 773 K for 0.5 h (s.o.), (iii) evacuation at 383 K for 0.5 h, (iv) reduction with CO in the range 393 to 773 K (generally at 623 K), (v) evacuation at 623 or at 673 K, and (vi) back-oxidation with O_2 at room temperature (RT) or at 773 K for 0.5 h. In some cases, CO-reduced catalysts were successively heated in water vapor at 973 K for 1 h in order to titrate the Cr(II) produced during the reduction with CO (*17*). All these titrations allowed the variation of the average oxidation number of chromium, $\bar{n}$, to be followed, and are expressed through electron acquisition (+) or loss (−) by means of the parameter e/Cr = (moles electrons/moles Cr atoms). During the s.o. treatment an increase of pressure was detected, whose extent was reproducible and significant especially in more concentrated catalysts, due to oxygen evolution (MS analysis), and therefore indicative of a decrease of $\bar{n}$. Extents of reduction, e/Cr, determined from CO consumed $(e/Cr)_{CO}$ were found to be systematically higher (5 to 10%) as compared to those determined from the CO_2 produced $(e/Cr)_{CO_2}$. Blank experiments on the pure ZrO_2 matrix showed that some CO was chemisorbed on the matrix without leading to reduction and that a fraction of CO_2, however small, was irreversibly adsorbed on the matrix even at 673 K. Unless otherwise specified, extents of reduction reported in the Results section are $(e/Cr)_{CO_2}$.

XPS Measurements

XPS spectra were obtained with a Leybold–Heraeus LHS 10 spectrometer interfaced to a Hewlett–Packard 2113 B computer. A twin anode, Al$K\alpha$ (1486.6 eV) and Mg$K\alpha$ (1253.6 eV) was employed, usually at 12 kV, 20 mA. The specimen treatment chamber was at 10^{-8} Torr, and the analysis chamber at 10^{-9} Torr or better. The sample, as fine powder, was pressed onto a gold-decorated tantalum plate attached to the sample rod, or could be transferred from a sealed tube, without exposure to air, from a separate gas treatment apparatus onto the sampling rod. The spectra were analyzed in the sequence Cr 2p, O 1s, C 1s, Zr 3d, to minimize the time of exposure to X-rays, for the first recording of Cr 2p region (about 7 min). Repeated scans after fixed times allowed following the possible influence of exposure to X-rays.

Zr 3d was taken as reference at 182.5 eV, and the absolute position of the peak was

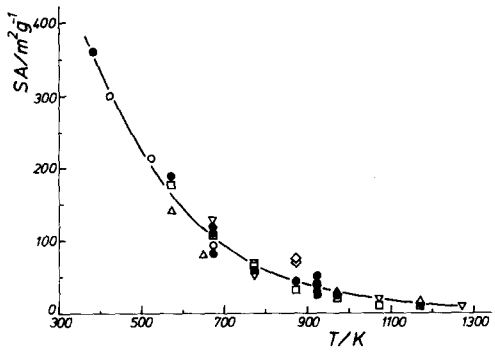

FIG. 2. Surface area (SA) for zirconium oxide samples vs heating temperature in air. Solid symbols from this study; open symbols from literature references: ○, Ref. (*44*); □, Ref. (*46*); △, Ref. (*47*); ▽, Ref. (*42*); ◇, Ref. (*48*).

found to be constant within ±0.2 eV. The data analysis procedure involved smoothing, nonlinear background subtraction and curve fitting (mixed Gaussian–Lorentzian functions).

RESULTS

Influence of Heat Treatment on ZrO_2

When ZrO_2(383) is subjected to heating in air at a given temperature T, its SA and textural properties change. The results obtained in several experiments are plotted in Fig. 2 as a function of temperature, together with those reported by other investigators for zirconia heated in comparable conditions. In addition to the temperature and time of heat treatment, other factors influence the SA value, such as water removal efficiency, the presence of impurities, and even (as tested in some experiments) total mass of the specimen, as further discussed under phase transformation of zirconia. On the whole, treatments in air tend to give lower SA values than in dry oxygen. A more marked influence is, however, exerted by heating in vacuum. To give a specific example, a ZrO_2(383) specimen calcined *in vacuo* at 773 K exhibits a BET SA of 121 m^2g^{-1} vs an average value (Fig. 2) of 70 m^2g^{-1}.

As regards the influence of heating in air on the pore structure of ZrO_2(383), Fig. 3A shows the evolution of the shape of the isotherm starting from 383 K and calcining in air for 5 h at 673 or 773 or 923 K. The ZrO_2(383) isotherm is the sum of Type I and Type IV in the BDDT classification (*18*), indicating the presence of micro- and mesopores. After a calcination at 673 or 773 K a Type IV isotherm is obtained, pointing out the prevailingly mesoporous character of the adsorbent. Finally, after calcination at 923 K the isotherm is still of Type IV but the shape and the starting point of the hysteresis loop reveal further collapse of the porous texture. The pore-size unimodal distribution found for ZrO_2(383) accordingly changes, as shown in Fig. 4A, with an increasing broadening around a maximum which shifts from about 1.3 to 9 nm.

The presence of micropores in the ZrO_2(383) sample is confirmed by the comparison between BET SA and S_t values: in fact, only in this case does the t-plot define a positive intercept (8 $cm^3_{NTP}\,g^{-1}$) on the V-axis, indicating microporosity (*19*), while for

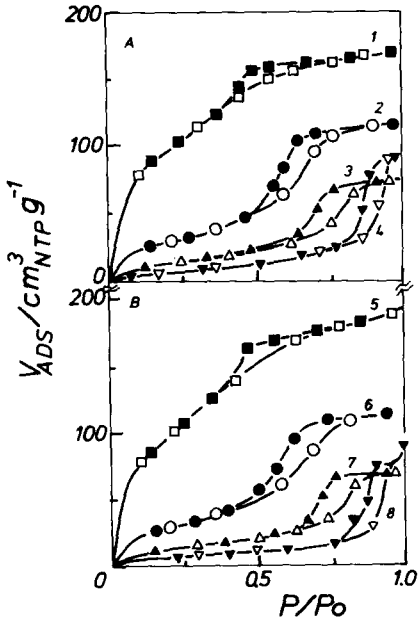

FIG. 3. N_2 adsorption isotherms at 77 K. (A) ZrO_2; (B) ZC samples. Open symbols, adsorption; solid symbols desorption. (1) ZrO_2(383)B; (2) ZrO_2(673)B; (3) ZrO_2(773)B; (4) ZrO_2(923)B; (5) ZC0.9(383)B; (6) ZC1.6(673)B; (7) ZC0.7(773)C; (8) ZC0.5(923)B.

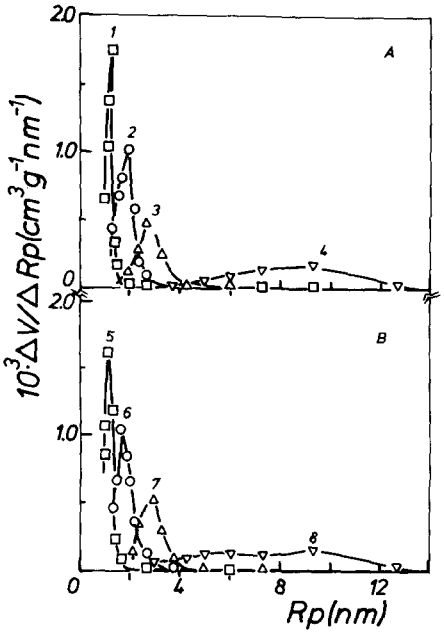

FIG. 4. Pore-size distributions. (A) ZrO_2; (B) ZC samples. Specimens numbered as in Fig. 3.

the remaining samples it extrapolates to the origin. Conversion of this volume to area covered by N_2 gives 35 m^2g^{-1}, which accounts for the discrepancy between the overestimated BET SA (360 m^2g^{-1}) and the corresponding S_t (323). The textural parameters for $ZrO_2(T)$ samples are summarized in Table 1.

Chromium Uptake by ZrO_2

Chromium uptake depends on the pH of the solution and on the previous heat treatment of zirconia. The uptake at pH 1 is larger than at pH 8, for any given pretreatment temperature T of $ZrO_2(T)$. The Cr uptake per gram decreases with increasing temperature pretreatment of zirconia, due to the decrease of SA. Since Cr uptake is a surface phenomenon, it is significant to consider the uptake per unit area as represented in Fig. 5, which shows the Cr uptake (Cr atoms/nm^2). The dashed line t (slope = 1) represents the adsorption of all Cr present in the solution (total adsorption). Curve a gives the results for samples based on $ZrO_2(383)$ at pH 1. Curve b embraces all other specimens based on $ZrO_2(T)$ at pH 1. Curve c refers to samples from $ZrO_2(773)$ at pH 8. The saturation value for $ZrO_2(923)$ is also reported. At pH 1 and at low Cr values, the uptake curve practically follows line t. The amount taken at pH 8 is considerably lower than that taken at pH 1. It is of interest to consider the limiting values of the different curves, which tend to level off. The values are about 2.5 Cr atoms/nm^2 for samples based on $ZrO_2(383)$ and 1.5 to 1.9 Cr atoms/nm^2 for all $ZCx(T \neq 383)$ specimens.

TABLE 1

Surface Areas and Pore Volumes of Pure Supports $ZrO_2(T)$

Calcination T (K)	BET SA (m^2g^{-1})	S_t (m^2g^{-1})	Pore volume (cm^3g^{-1})	Mesopore volume (cm^3g^{-1})
383	360	323	0.26	0.07
673	118	118	0.18	0.10
773	56	55	0.11	0.07
923	30	29	0.14	0.10

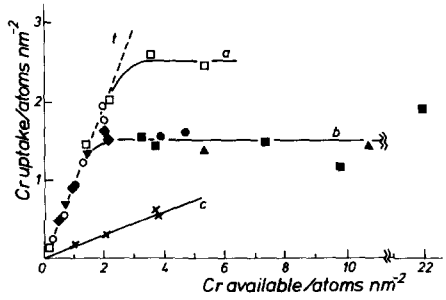

FIG. 5. Chromium uptake as a function of the Cr available in the solution, both expressed as Cr atoms per nm^2 of zirconia surface. Line (t), total adsorption. Curve (a), samples based on $ZrO_2(383)$ at pH 1: ○, ZCB; □, ZCE. Curve (b), samples based on $ZrO_2(T > 383)B$ at pH 1: ▼, (573); ◆, (673); ●, (773); ■, (923); ▲, (1023). Curve (c), x, samples based on $ZrO_2(773)C$ at pH 8.

Chlorine Content

As mentioned in the Experimental section, Cl is only eliminated with difficulty from the zirconia obtained via $ZrOCl_2$. Indeed, even if the liquid after filtration does not reveal the presence of Cl, analysis of the solid residue shows a Cl content which can

be as high as 2 wt%. To mention a specific example, a ZrO_2(383) specimen showed 3.5 wt% Cl after rinsing for 3 h, and 1.7 after 8 h (with no opalescence due to the AgCl precipitate test seen in the rinsing water). After 72 h also the solid residue was free from Cl.

Heating in air at 673 K eliminates Cl, but slowly. Thus, from an initial content of 3.5 wt%, the Cl content becomes 2.3% after 10 h, 0.8% after 92 h, and 0.6% after 140 h. Higher temperatures are required to remove Cl, and an oxygen atmosphere is more efficient than N_2. Thus (in parentheses, values for N_2 atmosphere), from an initial content of about 2 wt%, the Cl content after 0.5 h becomes 1.0 (1.3) at 773 K, 0.4 (0.9) at 873 K, 0.2 (0.4) at 973 K, and 0.1 (0.2) at 1073 K.

Chromium-containing specimens, ZCx (383), give a lower Cl content with respect to the starting ZrO_2 material. Thus, from an initial 2.3 wt% the Cl (wt%) was found to be 0.55 and 0.54 in two independent determinations of a ZC2(383)B specimen. The decrease can be accounted for by the concomitant action of two factors: (i) an effective additional rinsing by the contacting solution, and (ii) a substitution of Cr-containing species (at pH 1) for the surface chloride ion. It is also worth noting that, as for pure ZrO_2, the Cl content is strongly reduced by oxidation at high temperatures. Thus, the same specimen ZC1.7(383)B only showed traces of Cl ($\leq$0.05 % w) after about 10 s.o. cycles.

Heat Treatment of ZC Samples

Specimens based on ZrO_2(383), whose SA is 360 m^2g^{-1}, are considered first. Detailed analysis before and after heat treatments are reported for one set only, ZCx(383)B, in Table 2. Results on different preparations closely parallel those of set B. The Cr content (wt%) after drying at 383 K, Cr_{tot}^{383}, is given in column 2. Column 3 gives the surface Cr concentration, $Cr_{tot}^{383}(s)$. As mentioned above, treatment at 773 K in dry oxygen proved to be a good starting conditioning of materials to be tested for surface and catalytic properties. The results of the chemical analysis after s.o. are therefore examined and are reported for set B in Table 2. Column 4 gives the Cr content (wt%) after s.o., Cr_{tot}^{773}. The increase observed relative to column 2 is due to water loss, which can vary from sample to sample. Column 5 gives the Cr extracted by NaOH, $Cr_{extr.}^{773}$, as specified above, column 6 gives the Cr found in the solid residue after extraction, $Cr_{res.}^{773}$, while column 7 gives the sum (column 5) + (column 6), Cr_{sum}^{773}, and is in good agreement with total Cr (column 4). Column 8 gives the ratio (extractable Cr)/(total Cr); it is apparent that a large fraction is present as Cr(VI), although a consistent part of Cr(VI) initially present before s.o. has undergone a reduction at 773 K, the reduced fraction increasing with Cr content.

Specimens based on $ZrO_2(T)$ are reported in Table 3. The columns give in order: (1) the symbol, (2) the SA, and (3) the Cr content, wt%, of specimens subjected to heating in air (773 K, 5 h), Cr_{tot}^{773}. Columns 4, 5, and 6 give the Cr extracted, $Cr_{extr.}^{773}$, the Cr found in the solid residue, Cr_{res}^{773}, and their sum, Cr_{sum}^{773}, the last values showing good agreement with those of column 3. The ratio of Cr extracted to total Cr (column 4)/(column 6) is given in column 7. Finally, columns 8 and 9 list the surface concentrations as atoms/nm^2 for the total Cr, $Cr_{tot}^{773}(s)$, and the Cr extractable by NaOH, $Cr_{extr.}^{773}(s)$, respectively. In the calculation of the last two quantities allowance has been made for the Cr contribution, taken as $Cr_2O_7^{2-}$, to the weight of the specimen, considering the SA as due to the ZrO_2 component, over which the dichromate ion is anchored.

Influence of Cr on Zirconia Texture

Comparison of Figs. 3A and 3B and Figs. 4A and 4B shows that the Cr uptake has very little or no effect on the porous texture and SA of zirconia. The presence of Cr strongly influences the development of textural properties with temperature in comparison with the pure zirconia. The protective effect of the Cr addition on the

TABLE 2

Analytical Cr Contents for ZCx(383) Samples[a]

(1) Sample	(2) Cr^{383}_{tot} (wt%)	(3) $Cr^{383}_{tot}(s)$ (at. nm^{-2})	(4) Cr^{773}_{tot} (wt%)	(5) $Cr^{773}_{extr.}$ (wt%)	(6) $Cr^{773}_{res.}$ (wt%)	(7) Cr^{773}_{sum} (wt%)	(8) $(Cr^{773}_{extr.})/(Cr^{773}_{sum})$
ZC0.9(383)B	0.88	0.29	1.03	0.77	0.23	1.00	0.77
ZC1.7(383)B	1.68	0.56	2.14	1.61	0.48	2.09	0.77
ZC3.6(383)B	3.55	1.22	4.24	2.75	1.60	4.35	0.63
ZC5.0(383)B	5.00	1.78	5.98	3.62	2.30	5.92	0.61

[a] In $Cr^{\#}_{*}$, # designates the temperature of the treatment, 383 K or 773 K (standard oxidation), * indicates: tot = total, extr. = extractable with NaOH, res. = residue, sum = column (5) + column (6), (s) = surface.

SA of specimens based on ZrO_2(383) and heated in air at different temperatures is shown in Fig. 6. The dependence of the antisintering effect on Cr loading is evident especially for 773 and 873 K heating temperatures (open circles and squares). It is, however, worth noting that, even after calcination at 973 K (triangles), 1.6 wt% Cr or more opposes the textural collapse to such an extent that the SA is more than twice that of the ZrO_2(383) subjected to the same heating treatment.

A similar protective action is displayed by Cr for vacuum-heated samples. As an example, by heating a sample ZC1(383)B at 773 K *in vacuo*, the following set of data were obtained: SA(BET) = 172 m^2g^{-1}, S_f = 158 m^2g^{-1} and mesopore volume = 0.15 cm^3g^{-1}, compared with 121 m^2g^{-1}, 122 m^2g^{-1}, and 0.13 cm^3g^{-1} for the support, ZrO_2(383), subjected to the same treatment (773 K *in vacuo*).

The protection exerted by Cr against sintering is also apparent for specimens based on zirconia previously heated above 383 K, as illustrated in Fig. 7A. SA values are reported for portions of specimens ZrO_2(573) and ZrO_2(673), subjected to additional heating (5 h, air) at 673 or 773 or 873 K for ZrO_2(573) (open circles, curve a), and at 773 or 873 K for ZrO_2(673) (open squares, curve b, practically coinciding with a). The observed decrease of SA, which agrees with that expected by Fig. 2, can now be compared with that shown by Cr-containing specimens (full symbols) subjected to the same treatments. As Fig. 7A shows, the impregnation and heating (5 h, air) at the same temperature previously experienced by the support alone do not affect the SA value, as already stated. If portions of the specimen ZC (573) are now heated (5 h, air) at 673 or 773 or 873 K, the observed decrease of SA (full circles, curve a′) is remarkably less than that observed for pure zirconia. The same effect is still shown by ZC (673) (full squares, curve b′).

X-Ray Analysis

ZrO_2 appears amorphous, either as prepared or after heating in air (5 h) at $T < 673$

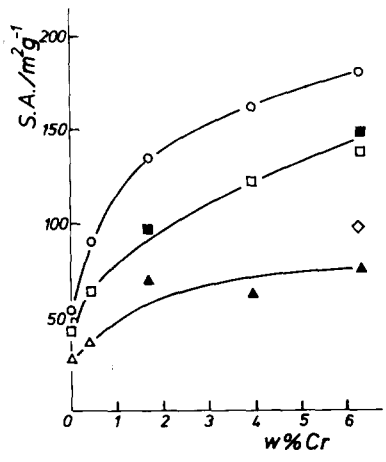

FIG. 6. Surface area vs Cr content of ZCx(383)E specimens heated in air: ○, 5 h 773 K; □, 5 h 873 K; △, 5 h 973 K; ■, 5 h 773 K + 5 h 873 K; ▲, 5 h 773 K + 5 h 873 K + 5 h 973 K; ◇, 5 h 873 K + 5 h 973 K.

TABLE 3

Analytical Cr Contents for ZCx(T > 383)) Samples[a]

(1) Sample	(2) SA (m^2g^{-1})	(3) Cr_{tot}^{773} (wt%)	(4) $Cr_{extr.}^{773}$ (wt%)	(5) $Cr_{res.}^{773}$ (wt%)	(6) Cr_{sum}^{773} (wt%)	(7) $(Cr_{extr.}^{773})/(Cr_{sum}^{773})$	(8) $Cr_{tot}^{773}(s)$ (at. nm^{-2})	(9) $Cr_{extr.}^{773}(s)$ (at. nm^{-2})
ZrO_2(923)B	40	—	—	—	—	—	—	—
ZrO_2(923)B	32	—	—	—	—	—	—	—
ZC1.0(573)B	175	0.96	0.72	0.26	0.98	0.73	0.65	0.48
ZC1.9(573)B	175	1.95	1.50	0.45	1.96	0.77	1.34	1.02
ZC1.0(673)B	119	0.96	0.70	0.26	0.96	0.73	0.95	0.69
ZC1.6(673)B	117	1.60	1.24	0.36	1.60	0.78	1.63	1.26
ZC0.4(923)B	32	0.39	0.33	0.07	0.40	0.83	1.42	1.21
ZC0.4(923)B*	32	0.40	0.33	0.07	0.40	0.83	1.46	1.20
ZC0.5(923)B	39	0.51	0.42	0.10	0.52	0.81	1.53	1.26
ZC0.5(923)B*	32	0.52	0.46	0.10	0.56	0.82	1.90	1.68
ZC0.3(1023)B	22	0.26	0.21	0.05	0.26	0.81	1.36	1.10
ZC0.3(1023)B*	22	0.27	0.21	0.06	0.27	0.78	1.43	1.10

[a] See Table 2 for explanation.

K. After treatments at $T > 673$ K, reflections of a mixture of tetragonal and monoclinic modifications is detected. The chromium-containing samples stay amorphous up to the higher temperatures with respect to undoped ZrO_2, and after crystallization has occurred the fraction of the m modification is lower in comparison with identically treated ZrO_2. The α-Cr_2O_3 reflections are detectable only after treatment at 1173 K, for samples ZC5.0(383)B and ZC5.8(383)A. It can be anticipated that the more sensitive ESR technique will disclose the presence of α-Cr_2O_3, but not below 973 K.

It is of interest to see the influence of Cr on the phase transformation t → m. As Fig. 8 shows, the fraction of tetragonal zirconia, f_t, is strongly increased by Cr addition for specimens based on ZrO_2(383) and heated at 773 or 873 or 973 K. The stabilization of the t phase is also observed for ZC specimens based on zirconia previously heated at 573 or 673 K. This is shown in Fig. 7B, which refers to the same specimens and treatment illustrated in Fig. 7A.

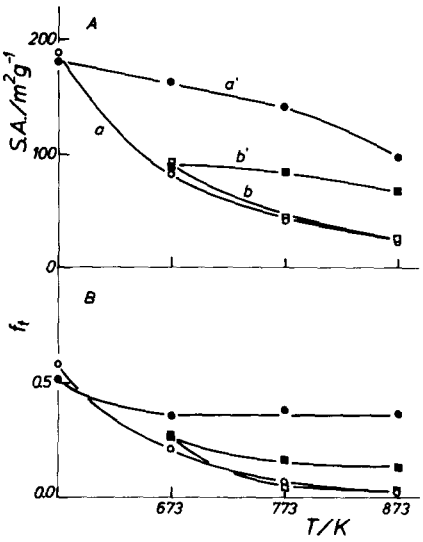

FIG. 7. (A) Surface area (SA) and (B) tetragonal fraction (f_t) vs heating temperature in air, 5 h. Samples: ○, ZrO_2(573)I; ●, ZC2.5(573)I; □, ZrO_2(673)I; ■, ZC1.3(673)I.

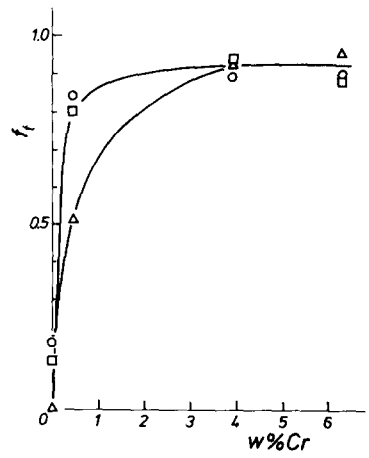

FIG. 8. Fraction of tetragonal zirconia (f_t) vs Cr content for ZrO_2(383)E and ZC(383)E samples heated in air (5 h) at: ○, 773 K; □, 873 K; △, 973 K.

DTA Measurements

The DTA curves show an endothermic effect in the temperature range 363–423 K due to water elimination, and an exothermic peak due to the ZrO_2 crystallization process. This last peak appears at about 723 K for pure ZrO_2, while for Cr-containing samples it is shifted to higher temperatures. As Fig. 9A shows, the shift increases with increasing chromium content. Figure 9B shows that the area of the peak, normalized to a 50-mg zirconia sample, is constant within the experimental error for the different samples if due allowance is made for the tail of the peak. It should also be noted that due to the high exothermicity of the process, the actual temperature experienced by a bulk calcination in the course of the preparation can be markedly higher than that of a small size specimen, with ensuing variation of SA in dependence of the size of the preparation.

Characterization by Redox Cycles

Values of the average oxidation state of *chromium*, $\bar{n}$, after the s.o. treatment, can be calculated from the chromium extracted with NaOH as Cr(VI), assuming the insoluble fraction to be in the 3+ state. Specifically: $n_{Cr_{extr.}} = 6\,x_{Cr_{extr.}} + 3\,(1 - x_{Cr_{extr.}})$, where

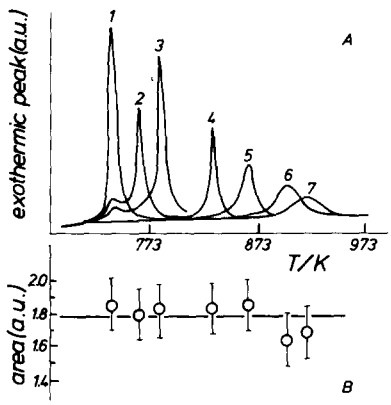

FIG. 9. (A) Exothermic features in DTA curves and (B) areas of the exothermic peaks, normalized to 50 mg of ZrO_2, for ZrO_2(383)A and ZCx(383)A samples: (1) ZrO_2; (2) ZC1; (3) ZC2; (4) ZC3.7; (5) ZC5; (6) ZC5.8; (7) ZC6.3.

$x_{Cr_{extr.}}$ is the molar fraction of Cr(VI) extracted with NaOH. The $n_{Cr_{extr.}}$ values are reported in column 2 of Table 4. A second method for the determination of $\bar{n}$ relies upon the oxygen released during the s.o. treatment, column 3 of Table 4. A satisfactory agreement between the two methods is found. With the exception of the sample ZC5.0(383)B, all n_{O_2} values (column 3) are in the range 5.4 to 5.6, in agreement with ESR results which indicate a constant Cr(V) content, 40 to 50%, in all ZC samples, again with the exception of the ZC5.0(383)B sample in which some Cr(III), in addition to Cr(VI) and Cr(V), is already present after the s.o. treatment (5).

The table also reports the e/Cr values determined from the CO consumed $(e/Cr)_{CO}$ (column 4) and the CO_2 produced $(e/Cr)_{CO_2}$ (column 5). Reasons why $(e/Cr)_{CO}$ values are higher than values of $(e/Cr)_{CO_2}$, making the latter values more reliable for evaluation of the extent of reduction, have already been mentioned. Accordingly, $\bar{n}$ values after reduction (n_{CO_2}, column 6) have been calculated as a difference: $n_{CO_2} = n_{O_2}-(e/Cr)_{CO_2}$, namely columns 3–column 5. Values of n_{O_2} are seen to be substantially constant (±0.1) and are consistent with nearly equal amounts of Cr(II) and Cr(III), the two species evidenced by means of ESR, IR, and XPS in ZC-reduced samples (5, 6). In agreement with the above assessment, the amount of Cr(II), as titrated with H_2O at 973 K, is about 50% of the total chromium $(e/Cr)_{H_2} = 0.5$ (column 7). Back-oxidation with O_2 at 773 K gives $(e/Cr)_{O_2}$ values (column 8) which are in good agreement with the $(e/Cr)_{CO_2}$ values of column (5), thus pointing to the reversibility of redox cycles on ZC samples.

XPS Analysis

The XPS results involve quantitative aspects, from which some morphological features can be deduced, and qualitative aspects of the different states of Cr in the course of the specimen treatments.

ZC(383). The spectrum in the Cr 2p region shows a feature which can be fitted by a single doublet $2p_{3/2} - 2p_{1/2}$. In the following,

TABLE 4

Average Oxidation Number ($\bar{n}$) of Chromium in Redox Cycles[a]

(1) Samples	(2) $\bar{n}_{Cr_{extr.}}$	(3) $\bar{n}_{O_2}$	(4) $(e/Cr)_{CO}$	(5) $(e/Cr)_{CO_2}$	(6) $\bar{n}_{CO_2}$	(7) $(e/Cr)_{H_2}$	(8) $(e/Cr)_{O_2}$
ZC0.9(383)B	5.3	5.4	3.1	3.0	2.4	0.5	3.0
ZC1.7(383)B	5.3	—	3.0	2.9	(2.4)	—	—
ZC5.0(383)B	4.8	4.8	2.6	2.4	2.4	0.5	2.4
ZC0.5(923)B	5.5	5.5	3.4	3.1	2.4	—	3.1
ZC0.5(923)B*	5.5	5.6	3.4	3.1	2.5	0.5	3.1

[a] See text for explanations.

reference to the 3/2 peak is made. Examination of 10 specimens of different Cr content leads to a BE value of 579.7 ± 0.4 eV and to a spin orbit separation ΔE_{SO} = 9.3 ± 0.2 eV. These values agree with the presence of Cr(VI). No other valency states of Cr could be identified, except after prolonged exposure to X-rays of concentrated specimens, leading to the appearance of a peak at BE = 576.5 eV, attributable to Cr(III).

The quantitative analysis is illustrated by Fig. 10, which shows the measured intensity ratio I(Cr)/I(Zr) as a function of the overall concentration ratio N(Cr)/N(Zr), where N represents the atomic concentration (atoms cm^{-3}) (solid symbols). In the same figure the calculated intensity ratios (crosses) are also reported, based on the sensitivity factors determined by us on the pure compounds Cr_2O_3, K_2CrO_4, and ZrO_2, which differ from those reported by Wagner *et al.* (*20*), but substantially agree with the intensity factors determined by the instrument producer (*21a*). A calculation of the intensity ratios based on the model of Kerkhof and Moulijn (*21b*) is also in agreement with the observed values. The results are indicative of a good dispersion throughout the zirconia volume.

ZC(T). The BE value of Cr is equal to that observed for ZC(383). The quantitative

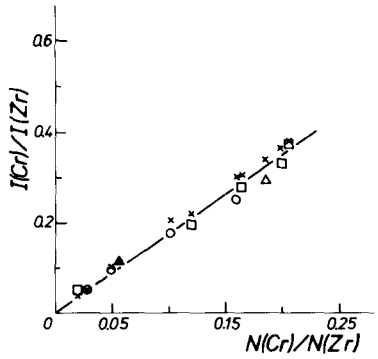

FIG. 10. Experimental (open symbols) and calculated (crosses) XPS intensity ratios I(Cr)/I(Zr) vs overall concentration ratio N(Cr)/N(Zr) for ZC(383) samples: ○, ZCB; △, ZCD; □, ZCE.

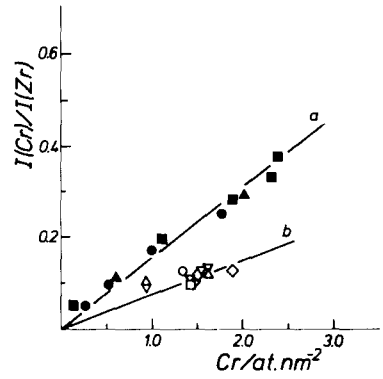

FIG. 11. XPS intensity ratios I(Cr)/I(Zr) vs surface Cr concentration. Curve a, samples based on ZrO_2(383): ●, ZCB; ▲, ZCD; ■, ZCE. Curve b, samples based on ZrO_2(T > 383): ○, ZC(573)B; △, ZC(673)B; ▽, ZC(773)C; ◇, ZC(923)B; □, ZC(1023)B.

asssessment of Cr presents some differences due to the absence of microporosity. It should in fact be noted that, in spite of the much lower Cr content by weight due to the lower SA values, the surface concentrations achieved are not much different. If specimens of equal surface concentration (Cr atoms/nm^2) are compared, the Cr peak intensity for ZC(923) is only about ½ of that of the ZC(383) specimens (Fig. 11). The factor ½ is due to the possibility of XPS "seeing" through the pore walls in the case of the (383) material (21b), a possibility no longer existing in the high-temperature treated materials (thicker walls).

ZC(T) after s.o. It is recalled that the Cr(V) concentration, as obtained from ESR measurements, is quite large, of the order of 40% of the total Cr concentration. Special efforts were therefore made to identify this species by XPS. The XPS analysis shows a change in the Cr(2*p*) features with a broadening towards lower BE values. The spectral interpretation requires the introduction of a component at about 1 eV lower BE than Cr(VI), which could be attributed to the presence of Cr(V). It is difficult to give a quantitative evaluation of the Cr(V) component, but a concentration of 50 ± 20% of the total is suggested. It is worth noting that

the intensity ratio $I(Cr)/I(Zr)$ is constant, pointing to the persistence of a good dispersion after s.o.

ZC(T) after CO reduction. The Cr 2*p* feature is markedly broadened (FWHM about 8 eV), and its BE, estimated by a rough single peak fitting, is shifted to lower values. In spite of the difficulties caused by the width and weakness of the feature, by appropriate curve fitting the presence of three components emerges: one at high BE, about 579.5 eV due to Cr(VI), caused by reoxidation of the specimen during handling and examination, a second component at 576.5 eV identified as Cr(III), and a third component at 575.5 eV due to Cr(II).

We note that it is the second case where an identification of the 2+ state for Cr has been made by XPS on supported catalysts, after the Cr/SiO_2 system reported by Best *et al.* (*22*) and more clearly by Merryfield *et al.* (*23*).

ZC(T), reduced by CO and oxidized by water at 743 K. The spectrum shows a shift to higher BE, with disappearance of the Cr(II) component, in agreement with the known chemistry of the system (*17*). The sequence (a) s.o.; (b) CO reduced; (c) H_2O vapour at 743 K is shown in Fig. 12, curves a to c, respectively.

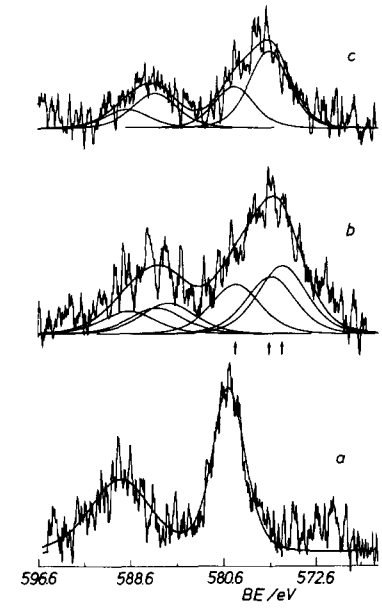

FIG. 12. Cr(2*p*) XPS region for ZC0.4(923)B sample: (a) after O_2 at 773 K; (b) from (a) plus CO at 623 K; (c) from (b) plus H_2O at 743 K. In spectrum (b) the arrows point to the Cr(VI), Cr(III) and Cr(II) positions.

DISCUSSION

The potential influence of the support on the properties (dispersion, chemical state, structure) of the active component has been indicated in the Introduction. In turn, the active component can affect some morphological features of the support relevant to the catalytic process, such as surface area and porosity, as well as ion exchange and adsorption capacities. In the following, attention is mainly given to the zirconia support and to the influence of chromium species on the properties of zirconia. The state and the change of the chromium component during thermal treatments is only briefly commented on, leaving the discussion and assessment of the present species to the papers devoted to the ESR and IR analysis (*6*).

Textural Features of Zirconia and the Effect of Cr Addition

The surface area of zirconia depends on the temperature of treatment and on the atmosphere. With due consideration of these parameters, as shown under Results, it is possible to prepare a support of given textural features, from high SA and micro-/mesoporous texture, to low SA and meso-/macroporous texture. The presence of chromium greatly affects the surface properties of either $ZrO_2(383)$ or $ZrO_2(T)$ (with $T > 383$) upon heating, exerting a protective effect against sintering and delaying the crystallization process. It is relevant that the tetragonal modification of zirconia is, to a very large extent, preserved in the presence of chromium.

Due to the adsorptive peculiarities of $ZrO_2(383)$, "hydrous zirconia," some properties of this material are examined first.

$ZrO_2(383)$. Hydrous zirconia, written also as $ZrO_2 \cdot xH_2O$ (*24, 25*) was found by us to

have a water content varying from about 13 wt% to 23 wt%, according to aging, impurity content, and time of storage. A content of about 11 wt% has been proposed by Clearfield (*26*), who also gives evidence for locating most of the OH groups on the surface. A full coverage of the surface of ZrO_2 particles of about 3 to 4 nm, corresponding to SA values of the order of 350 m^2g^{-1} (as found, Fig. 2) would give a weight loss of about 10 wt% if an OH surface density of about 9.4/nm^2 is assumed, corresponding to the most dense plane of ZrO_2 (t). Hence, a weight loss of 10 to 23 wt% corresponds to 1 to 2.3 monolayers. Holmes *et al.* (*27*) also state that about 2.3 monolayers of hydroxide are present on the surface.

The hydrous zirconia is amorphous to X-rays, but Livage *et al.* (*28*) and Keramidas and White (*29*) give evidence for a tetragonal type of structure in the amorphous material. This deduction also accords with the stabilization of the t form in small size crystals (for a discussion and references see Garvie and Swain (*30*), Heuer and Rühle (*31*), and Dow Witney (*32*)). It is also recalled that adsorbed Cl^- ions contribute to the stabilization of the t form (*33*). The type of exposed planes can be hypothesized from the general principle of low index planes being favored. This is indeed so for the related m structure, where a preferential exposure of (111), (110), and (100) faces was found by Warble (*34*). Finally, the equivalence of particle size with crystallite size up to a treatment at 1073 K was shown by Itoh (*35*). All these observations allow describing ZrO_2(383) as composed of tetragonal-like crystals whose exposed (111), (110), and (100) planes are the bounding faces coming into contact with the solution.

ZC(383). The stabilizing effect of additives against sintering, as observed for Cr addition (Fig. 6), is per se an indication of a strong interaction with the support, which will manifest itself also in the changes in the Cr species. A similar observation has been made by Turlier *et al.* (*36*) for yttria and lanthana additions. Further evidence of a strong interaction between Cr species and zirconia is the shift of the crystallization peak in DTA. The influence of the surface chemistry of microcrystals on the crystallization process has been invoked by most investigators, and the surface energy term is clearly exerting an important role and could explain the stabilization of the t form at low temperatures.

The surface energy term can be affected by the interaction with Cr species (chromate and dichromate), and the stabilization of the t form upon Cr addition could find an explanation along this line. On the other hand, within the experimental error, no large difference in the amount of the crystallizing material is found on increasing the Cr content (Fig. 9), thereby confirming that stabilization of the X-ray amorphous microcrystals is taking place. Relevant to the present case are the data reported by this laboratory on the influence of additives Cl^-, ReO_4^-, Ti(IV) to ZrO_2(383) on some solid state and surface chemistry properties (*37*). On those same grounds the interaction of Cr(VI) with zirconia can also be classified as strong.

The Cr Uptake Process. The Cr uptake by the zirconia from the solution is the first step of the sequence leading to the formation of the supported catalysts. It is important, as often noted (e.g., Brunelle (*38*), Knözinger (*39*)), to describe this step in order to justify and understand the attained loadings. In view of the strength of the interaction, a chemical reaction must occur between the Cr(VI) species in solution and the surface of zirconia. Based on a tetragonal model, as noted before, a density of Zr atoms/nm^2 is calculated as: plane (100), 5.2; plane (001), 7.5; and plane (011), 9.4; all with Teufer's cell (*16*). The positive surface sites formed in an acid medium and interacting with the Cr-containing anions can be written as $S\text{–}OH_2^+$. An upper limit of the adsorbable anions, in the unrealistic hypothesis that all Zr atoms exposed are transformed, via Zr–OH to $Zr\text{–}OH_2^+$, would thus correspond to the above figures for a monodentate attachment. The effective density, however,

will be controlled by several factors, including the strength of surface acid sites and the stability of the resultant adduct. The situation encountered in γ-Al_2O_3 is significant in this context, for which a full coverage by OH groups is attained and is indeed essential for its stability (*40*), and yet not all groups have equal chemical and exchange behavior (*41*). It is important to note that in an acid medium well below the isoelectric point (IEP) of zirconia (stated as between 4 and 4.9 by Crucean and Rand (*42*), who question the higher values (*43*) (see however *44*)), uptake of anions is favored. Attention is thus drawn to the exchange capacity toward anions. The simple geometry, unique charge, and strength render the Cl^- adsorption studied by Inoue and Yamazaki (*44*) particularly significant. The authors found a decrease of Cl^- uptake with increasing temperature of zirconia pretreatment. If the SA variation is taken into account, a leveling of the Cl^- uptake to about 1.8 Cl^- ions/nm^2 can be calculated. Our results give a maximum loading of roughly 1.6 Cr atoms/nm^2, for a zirconia treated at or above 573 K. The two figures are in sufficient agreement to suggest a crude approximation based on electrostatic considerations. As shown, the coverage corresponds to about $\frac{1}{4}$ of the geometrical sites, pointing to an occupancy that leaves free the sites next to each occupied site. A more complete treatment should take into account other arguments and factors such as stability constants of the adduct, and variation of the strength of the surface acid sites. On the whole, however, thermally treated zirconia presents itself as a suitable support because of its maintained capacity of interaction with the precursors of the active component and of its textural stability.

The hydrous zirconia has a reproducible behavior if due attention is paid to the preparation method. While it is subject to marked textural and structural change upon heating, its high exchange capacity is of interest for the preparation of doped high-temperature materials.

The ZrO_2(383) material also lends itself to a comparison of exchange capacity between Cr species and Cl^- (*44*). From Figs. 7 (Cl uptake) and 6 (SA values of the quoted Ref. (*44*)), it can be inferred that the exchange capacity of a 383 K treated material would be about 2.5 Cl^- atoms/nm^2. This value closely corresponds to the saturation value of the same material in Fig. 5 of the present report. It should also be noted that the material reported here and that studied by Inoue and Yamazaki (*44*) are comparable not only for the method of preparation, but also for the SA values and for the weight loss registered. If the ion exchange capacity is regarded as the amount of the adsorbed species necessary to neutralize the charge of the sites with an opposite sign, and given the equivalence (2.5 Cr at/nm^2) found by us and the fact that Cl^- acts as a singly charged anion, one infers that the charge associated with one Cr atom must be -1 for each neutralized site, s^+. This gives rise to two possibilities: either the attachment of $HCrO_4^-$, a species dominant at low Cr concentration, to a single s^+, or a bidentate attachment of a dichromate ion $Cr_2O_7^{2-}$ to two s^+, the $Cr_2O_7^{2-}$ hypothesis being consistent with the expected Cr species in acid solution at elevated Cr concentrations (*45*), such as those used for high Cr content in ZC(383).

Stabilization of Cr Oxidation States

The similarity of behavior of ZC(T), irrespective of the zirconia pretreatment temperature T, toward the evolution of the Cr states, discloses a characteristic surface chemistry of the zirconia, not only toward the adsorption of chromium species (Fig. 5) but also in the stabilization of Cr species. A short discussion of some features is given below.

A first observation refers to the marked tendency of Cr(VI) to reduce to Cr(V) at 773 K in oxygen. By comparison with the CrO_x/SiO_2 system, the Cr(V) state is much more stable on zirconia. The observed reversibility and reproducibility (Table 4) guarantee that the stability of Cr(V) is a feature im-

parted by the support and common to a wide range of Cr concentrations and of zirconia pretreatment temperatures.

A second observation refers to the reduction by CO at 623 K, which, though giving rise to a substantial amount of Cr(II), always leaves about $\frac{3}{4}$ or more of Cr(III) (Table 4). A stabilization of Cr(III) in comparison with the CrO_x/SiO_2 system is therefore deduced.

However, statement of the oxidation number, as in Cr(III), is not sufficient to mark the species present on the surface. In fact, in comparison with the CrO_x/SiO_2 system, a less easy evolution toward Cr_2O_3 is observed over zirconia, as witnessed by the maintenance of a good dispersion of Cr(III) species, by the reversibility of the cycle, and by the high temperatures required to identify the presence of α-Cr_2O_3 by X-rays, and even by ESR. This protection against sintering of chromia is an important feature of zirconia, relevant to its properties as a catalyst support.

We conclude with a final observation. The stabilization of both dispersed Cr(V) and Cr(III) species is suggestive of a redox correlation between states (V) and (III). Substantiation of this hypothesis can only be given by a deeper insight into the structure of the Cr surface species and their changes, which will be possible after the ESR characterization presented in Part II.

CONCLUSIONS

Zirconia as a support is capable of adsorbing chromium species with a strong interaction, responsible for a mutual influence on the textural and chemical properties observed upon heat treatments. On one hand, the zirconia support is protected against sintering and phase transformation from the low-temperature metastable tetragonal to the stable monoclinic form. On the other hand, Cr(V) species are stabilized. If reduced, Cr(III) and Cr(II) species are formed. Cr(II) is selectively oxidized to Cr(III) by H_2O vapor at high temperature. By oxygen treatment, Cr(VI) and Cr(V) are restored, and the redox behavior can be reproduced.

The tendency of Cr(III) to aggregate and to evolve toward α-Cr_2O_3 is hindered by the support. Thus, a dispersed form of Cr(III) and Cr(II), or of Cr(III), can be achieved.

REFERENCES

1. McDaniel, M. P., *Adv. Catal.* **33,** 47 (1985).
2. (a) Myers, D. L., and Lunsford, J. H., *J. Catal.* **99,** 140 (1986). (b) Lunsford, J. H., Fu Shi-Liang and Myers, D. L., *J. Catal.* **111,** 231 (1988).
3. Grünert, W., Shpiro, E. S., Feldhaus, R., Anders, K., Antoshin, G. V., and Minachev, Kh. M., *J. Catal.* **100,** 138 (1986).
4. Ghiotti, G., Garrone, E., and Zecchina, A., *J. Mol. Catal.* **46,** 61 (1988).
5. Cimino, A., Cordischi, D., De Rossi, S., Ferraris, G., Gazzoli, D., Indovina, V., Minelli, G., Occhiuzzi, M., and Valigi, M., *in* "Proceedings 9th Int. Congr. Catal." (Calgary 1988) (M. J. Phillips and M. Ternan, Eds.), Vol. 3, p. 1465. Chem. Inst. Canada, Ottawa (1988).
6. Cimino, A., Cordischi, D., Febbraro, S., Gazzoli, D., Indovina, V., Occhiuzzi, M., Valigi, M., Boccuzzi, F., Chiorino, A., and Ghiotti, G., *J. Mol. Catal.* **55,** 23 (1989).
7. Li Wang and Hall, W. K., *J. Catal.* **77,** 232 (1982).
8. Kolthoff, M. I., and Lingane, J. J., *J. Amer. Chem. Soc.* **57,** 2126 (1935).
9. Cotton, F. A. and Wilkinson, G., "Advanced Inorganic Chemistry," 2nd ed., p. 859. Interscience, New York (1968).
10. Charlot, G. "Les Méthodes de la Chimie Analytique. Analyse Quantitative Minérale," p. 703. Masson, Paris (1961).
11. Ref. (*10*), p. 702.
12. Brunauer, S., *Chem. Eng. Prog. Symp. Ser.* **65,** 1 (1969).
13. Gregg, S. J., and Sing, K. S. W., "Adsorption, Surface Area and Porosity," 2nd ed., p. 113. Academic Press, London (1982).
14. Lippens, B. C., and de Boer, J. H., *J. Catal.* **4,** 319 (1965).
15. Lecloux, A., and Pirard, J. P., *J. Colloid Interface Sci.* **70**(2), 265 (1979).
16. Teufer, G., *Acta Crystallogr.* **15,** 1187 (1962).
17. Lugo, H. J., and Lunsford, J. H., *J. Catal.* **91,** 155 (1985).
18. Brunauer, S., Deming, L. S., Deming, W. S., and Teller, E., *J. Amer. Chem. Soc.* **62,** 1723 (1940).
19. Ref. (*13*), p. 210.
20. Wagner, C. D., Davies, L. E., Zeller, M. V., Taylor, J. A., Raymond, R. H., and Gale, L. H., *Surf. Interface Anal.* **3,** 211 (1981).

21. (a) Berresheim, K., Leybold-Heraeus, private communication; (b) Kerkhof, F. P. J. M., and Moulijn, J. A., *J. Phys. Chem.* **83**(12), 1612 (1979).
22. Best, S. A., Squires, R. G., and Walton, R. A., *J. Catal.* **47,** 292 (1977).
23. Merryfield, R., McDaniel, M., and Parks, G., *J. Catal.* **77,** 348 (1982).
24. Rijnten, H. Th., *in* "Physical and Chemical Aspects of Adsorbents and Catalysts" (B. G. Linsen Ed.), pp. 315–372. Academic Press, New York (1970.
25. Gimblett, F. G. R., Rahman, A. A., and Sing, K. S. W., *J. Colloid Interface Sci.* **84,** 337 (1981).
26. Clearfield, A., *Inorg. Chem.* **3,** 146 (1964).
27. Holmes, H. F., Fuller, E. L., and Beh, R. A., *J. Colloid Interface Sci.* **47,** 365 (1974).
28. Livage, J., Doi, K., and Mazières, C., *J. Amer. Ceram. Soc.* **51,** 349 (1968).
29. Keramidas, V. G., and White, W. B., *J. Amer. Ceram. Soc.* **57,** 22 (1974).
30. Garvie, R. C., and Swain, M. V., *J. Mater. Sci.* **20,** 1193 (1985).
31. Heuer, A. H., and Rühle, M., *Acta Metall.* **33,** 2101 (1985).
32. Dow Whitney, E., *Trans. Faraday Soc.* **61,** 1991 (1965).
33. Blesa, M. A., Maroto, A. J. G., Passaggio, S. I., Figliola, N. A., and Rigotti, G., *J. Mater. Sci.* **20,** 4601 (1985).
34. Warble, C. E., *Ultramicroscopy* **15,** 301 (1984).
35. Itoh, T., *J. Mater. Sci. Lett.*, **4,** 431 (1985).
36. Turlier, P., Dalmon, J. A., Martin, G. A., and Vergnon, P., *Appl. Catal.* **29,** 305 (1987).
37. Valigi, M., Cimino, A., Gazzoli, D., and Minelli, G., *Solid State Ionics* **32/33,** 698 (1989).
38. Brunelle, J. P., *Pure Appl. Chem.* **50,** 1211 (1978).
39. Knözinger, H., *in* "Catalysis by Acids and Bases" (B. Imelik *et al.*, Eds.), p. 111. Elsevier, Amsterdam (1985).
40. Soled, S., *J. Catal.* **81,** 252 (1983).
41. Knözinger, H., and Ratnasamy, P., *Catal. Rev.* **17,** 31 (1978).
42. Crucean, E., and Rand, B., *Trans. J. Brit. Ceram. Soc.* **78,** 96 (1979).
43. Parks, G. A., *Chem. Rev.* **65,** 177 (1965).
44. Inoue, Y., and Yamazaki, H., *Bull. Chem. Soc. Japan* **60,** 891 (1987).
45. Kelsall, G. H., House, C. I., and Gudyanga, F. P., *J. Electroanal. Chem.* **244,** 179 (1988).
46. Tanabe, K., *Mater. Chem. Phys.* **13,** 347 (1985).
47. Otero Arean, C., Villa Garcia, M. A., and Fernandez Colinas, J. M., *Mater. Chem. Phys.* **13,** 163 (1985).
48. Bird, R., Kemball, C., and Leach, H. F., *J. Chem. Soc. Faraday Trans. 1* **83,** 3069 (1987).